

# Understanding oscillating features of the time-like nucleon electromagnetic form factors within the extending vector meson dominance model

Bing Yan,<sup>1,2</sup> Cheng Chen,<sup>1,3</sup> Xia Li,<sup>2</sup> and Ju-Jun Xie<sup>1,3,4,\*</sup>

<sup>1</sup>*Institute of Modern Physics, Chinese Academy of Sciences, Lanzhou 730000, China*

<sup>2</sup>*College of Mathematics and Physics, Chengdu University of Technology, Chengdu 610059, China*

<sup>3</sup>*School of Nuclear Sciences and Technology, University of Chinese Academy of Sciences, Beijing 101408, China*

<sup>4</sup>*Southern Center for Nuclear-Science Theory (SCNT), Institute of Modern Physics, Chinese Academy of Sciences, Huizhou 516000, Guangdong Province, China*

We investigate the nonmonotonic behavior observed in the time-like nucleon electromagnetic form factors. Using a phenomenological extending vector meson dominance model, where the ground states  $\rho$  and  $\omega$  and their excited states  $\rho(2D)$ ,  $\omega(3D)$ , and  $\omega(5S)$  are taken into account, we have successfully reproduced the cross sections of  $e^+e^- \rightarrow p\bar{p}$  and  $e^+e^- \rightarrow n\bar{n}$  reactions. Furthermore, we have derived the nucleon electromagnetic form factors in the time-like region, and it is found that the so-called periodic behaviour of the nucleon effective form factors is not confirmed. However, there are indeed nonmonotonic structures in the line shape of nucleon effective form factors, which can be naturally reproduced by considering the contributions from the low-lying excited vector states.

## I. INTRODUCTION

Nucleons (proton and neutron) are composite particles consisting of three valence quarks ( $uud$  and  $udd$ ) and a neutral sea of strong interaction. Despite the discovery of the proton over 100 years ago, an exact theoretical description of its internal structure has not been achieved within the framework of quantum chromodynamics (QCD) theory. This is due to the non-perturbative nature of QCD in the energy regime of the nucleon. On the theoretical side, the nucleon electromagnetic structure can be described by the electromagnetic form factors (EMFFs), which depends on squared of the four-momentum ( $q^2$ ) of the exchanged virtual photon. The EMFFs in the space-like region ( $q^2 < 0$ ) are real and they can be associated with the charge and magnetic distribution of the nucleons [1]. However, in the time-like region ( $q^2 > 0$ ), the EMFFs become complex, providing information on the time evolution of the nucleon's charge and magnetic moments at the nucleon-antinucleon pair formation point [2–5]. On the experimental side, the EMFFs of nucleons were measured by both the  $e^-N \rightarrow e^-N$  elastic scattering [6–10] and  $e^+e^- \rightarrow N\bar{N}$  annihilation reactions [11–20]. One can obtain the space-like form factors from the former process and the time-like form factors from the latter process, respectively.

Traditionally, most experimental data on electromagnetic form factors have been collected in the space-like region through electro-proton elastic scattering. However, a new era has begun with the introduction of electron-positron annihilation reactions [21–23], where a nucleon-antinucleon pair is formed by a virtual photon.

Over the past decade, the BESIII Collaboration has made significant advancements in studying the timelike effective form factors of nucleons. Within the theoretical formula proposed in Refs. [4, 5], it is found that not only the effective form

factor of proton, but also the effective form factor of neutron has the periodic structures after subtracting a dipole or modified dipole contributions [18], leading to the discovery of an intriguing phenomenon known as oscillation behavior. This phenomenon has been further confirmed by recent measurements conducted by the SND Collaboration [20]. However, these new measurements conflict with previously fitted results in the energy region below 2 GeV.

A comprehensive analysis of the nucleon's electromagnetic form factors in both the space- and time-like regions using dispersion theory is conducted in Ref. [24]. For the periodic behaviour of the nucleon's electromagnetic form factors, it has been studied in Refs. [25–33], using various phenomenological methods. It is worthy mentioning that the periodic behaviour of the nucleon's electromagnetic form factors are induced by those broad vector mesons according to the studies in Ref. [25]. However, these vector mesons couple to  $N\bar{N}$  pair very weakly. In fact, a unified description of the time- and space-like electromagnetic form factors of nucleons was proposed in Ref. [34], where these low-lying vector mesons were taken into account. Meanwhile, in the time-like region, a revised Breit-Wigner formulas with momentum-dependent widths are needed for these vector resonances [34]. Indeed, the contributions of these vector mesons are important to the reactions of  $e^+e^-$  annihilation into light hadrons [35–43].

The vector meson dominance (VMD) model is a successful approach for studying the baryon EMFFs, in both space-like and time-like regions [44–47]. And, within the vector meson dominance model for studying the electromagnetic form factors of baryons, there is a phenomenological intrinsic form factor  $g(s)$ , which is a characteristic of valence quark structure. From these studies of the nucleon and hyperon EMFFs [44–50], it is found that a better choice of  $g(s)$  is the dipole form

$$g(s) = \frac{1}{(1 - \gamma s)^2}, \quad (1)$$

with  $\gamma = 1.41 \text{ GeV}^{-2}$  for the case of nucleon.

\*Electronic address: xiejujun@impcas.ac.cn

On the other hand, the BESIII Collaboration has also provided a large number of experimental data about  $e^+e^-$  annihilation into light mesons [35–43], which provides the basis for our construction of light vector states. From the analyses of the  $e^+e^- \rightarrow \pi^+\pi^-$ ,  $\omega\pi^0$ , and  $\rho^0\eta'$  reactions, these  $\rho$  excited states were studied in Refs. [51–53]. The spectrum of excited  $\rho$ ,  $\omega$ , and  $\phi$  states were also investigated in Ref. [54] using the modified Godfrey-Isgur model [55]. By performing the phenomenological analysis, the two-body strong decay of the excited  $\rho$  states are systematically studied [56]. Based on the above theoretical calculations and the vector mesons listed in the particle data group (PDG) [57], we take  $\rho(2D)$ ,  $\omega(3D)$ , and  $\omega(5S)$  into account in this work. Their masses and widths are collected in Table I. By considering the contributions of these above low-lying vector meson excited states, we studied the  $e^+e^- \rightarrow p\bar{p}$  and  $e^+e^- \rightarrow n\bar{n}$  reactions within the VMD model. It is found that the total cross sections of the two above reactions (corresponding to the nucleon's effective form factors) and the nucleon electromagnetic form factors can be well described. However, the so-called oscillation behavior of the nucleon's EMFFs discovered by the BESIII Collaboration [18] is not confirmed.

TABLE I: Masses and widths of the excited vector states used in this work.

State	Mass (MeV)	Width (MeV)	Reference
$\rho(2D)$	2040	202	[52, 56]
$\omega(3D)$	2283	94	[53]
$\omega(5S)$	2422	69	[53]

This article is organized as follows: in the next section, we show the theoretical formalism of the nucleon's EMFFs in the VMD model. Numerical results of the nucleon's effective form factors, the total cross sections of  $e^+e^- \rightarrow p\bar{p}$  and  $e^+e^- \rightarrow n\bar{n}$  reactions, and the oscillating features of the nucleon's EMFFs are shown in Sec. III. A short summary is given in the last section.

## II. THEORETICAL FORMALISM

Under the one photon exchange approximation, the total cross section of the reaction  $e^+e^- \rightarrow N\bar{N}$  can be expressed in terms of the effective form factor  $|G_{\text{eff}}(s)|$  as [58–60]

$$|G_{\text{eff}}(s)| = \sqrt{\frac{2\tau|G_M(s)|^2 + |G_E(s)|^2}{1 + 2\tau}}, \quad (2)$$

$$\sigma_{e^+e^- \rightarrow N\bar{N}} = \frac{4\pi\alpha^2\beta C_N}{3s} \left(1 + \frac{1}{2\tau}\right) |G_{\text{eff}}(s)|^2, \quad (3)$$

with  $\alpha = e^2/(4\pi)$  the fine-structure constant and  $\beta = \sqrt{1 - 4m_N^2/s}$  the phase-space factor,  $m_N$  is the nucleon mass. Here,  $C_N$  represents the S-wave Sommerfeld-Gamow factor accounts for the electromagnetic interaction of charged pointlike fermion pairs in the final state [61]. For proton,  $C_p = y/(1 - e^{-y})$  with  $y = \frac{\alpha\pi}{\beta} \frac{2M_p}{\sqrt{s}}$ , while for the neutron,  $C_n = 1$ . Considering the  $C_N$  factor, it is expected that the

total cross section of  $e^+e^- \rightarrow p\bar{p}$  reaction is nonzero at the reaction threshold.

Based on parity conservation and Lorentz invariance, the electromagnetic form factors of the baryons with spin of 1/2 can be characterized by two independent scalar functions  $F_1(q^2)$  and  $F_2(q^2)$  depending on  $q^2$ , which are called the Dirac and Pauli form factors, respectively. The electrical and magnetic form factors of nucleon can be written as [62–64],

$$G_E(q^2) = F_1(q^2) + \tau F_2(q^2), \quad (4)$$

$$G_M(q^2) = F_1(q^2) + F_2(q^2), \quad (5)$$

where  $\tau = q^2/(4m_N^2)$  and  $q^2 = s$  the invariant mass square of the  $e^+e^-$  annihilation process. Once we have  $F_1(s)$  and  $F_2(s)$ , we can naturally obtain the electromagnetic form factors of the nucleon. Then the total cross sections of  $e^+e^- \rightarrow N\bar{N}$  can be easily calculated.

Because proton and neutron are isospin doublets, the  $p\bar{p}$  and  $n\bar{n}$  states are expressed in terms of isospin 0 and 1 components. The mixtures of isovector and isoscalar for  $p\bar{p}$  and  $n\bar{n}$  of equal relative weight but different signs are imposed by the isospin symmetry as introduced by the underlying Clebsch-Gordan coefficients. As discussed above, in addition to these ground isovector  $\rho$  meson and isoscalar  $\omega$  meson, we also consider the excited vector mesons with masses around 2.0 to 3.0 GeV.<sup>1</sup>

Then, the Dirac and Pauli form factors  $F_1$  and  $F_2$  for nucleon in the time-like region can be parameterized as,

$$F_1^n = g(s) \left( f_1^n - \frac{\beta_\rho}{\sqrt{2}} B_\rho - \frac{\beta_{\rho(2D)}}{\sqrt{2}} B_{\rho(2D)} + \frac{\beta_\omega}{\sqrt{2}} B_\omega + \frac{\beta_{\omega(3D)}}{\sqrt{2}} B_{\omega(3D)} + \frac{\beta_{\omega(5S)}}{\sqrt{2}} B_{\omega(5S)} \right), \quad (6)$$

$$F_2^n = g(s) \left( f_2^n B_\rho - \frac{\alpha_{\rho(2D)}}{\sqrt{2}} B_{\rho(2D)} + \frac{\alpha_\omega}{\sqrt{2}} B_\omega + \frac{\alpha_{\omega(3D)}}{\sqrt{2}} B_{\omega(3D)} + \frac{\alpha_{\omega(5S)}}{\sqrt{2}} B_{\omega(5S)} \right), \quad (7)$$

$$F_1^p = g(s) \left( f_1^p + \frac{\beta_\rho}{\sqrt{2}} B_\rho + \frac{\beta_{\rho(2D)}}{\sqrt{2}} B_{\rho(2D)} + \frac{\beta_\omega}{\sqrt{2}} B_\omega + \frac{\beta_{\omega(3D)}}{\sqrt{2}} B_{\omega(3D)} + \frac{\beta_{\omega(5S)}}{\sqrt{2}} B_{\omega(5S)} \right), \quad (8)$$

$$F_2^p = g(s) \left( f_2^p B_\rho + \frac{\alpha_{\rho(2D)}}{\sqrt{2}} B_{\rho(2D)} + \frac{\alpha_\omega}{\sqrt{2}} B_\omega + \frac{\alpha_{\omega(3D)}}{\sqrt{2}} B_{\omega(3D)} + \frac{\alpha_{\omega(5S)}}{\sqrt{2}} B_{\omega(5S)} \right), \quad (9)$$

<sup>1</sup> It's worth noting that due to the Okuba-Zweig-lizuka rule, we do not consider the  $\phi$  meson and its excited states here.

with

$$B_\rho = \frac{m_\rho^2}{m_\rho^2 - s - im_\rho\Gamma_\rho}, \quad (10)$$

$$B_\omega = \frac{m_\omega^2}{m_\omega^2 - s - im_\omega\Gamma_\omega}, \quad (11)$$

$$B_{\rho(2D)} = \frac{m_{\rho(2D)}^2}{m_{\rho(2D)}^2 - s - im_{\rho(2D)}\Gamma_{\rho(2D)}}, \quad (12)$$

$$B_{\omega(3D)} = \frac{m_{\omega(3D)}^2}{m_{\omega(3D)}^2 - s - im_{\omega(3D)}\Gamma_{\omega(3D)}}, \quad (13)$$

$$B_{\omega(5S)} = \frac{m_{\omega(5S)}^2}{m_{\omega(5S)}^2 - s - im_{\omega(5S)}\Gamma_{\omega(5S)}}. \quad (14)$$

Here, we take  $m_\rho = 775.26$  MeV,  $\Gamma_\rho = 147.4$  MeV,  $m_\omega = 782.66$  MeV, and  $\Gamma_\omega = 8.68$  MeV. In addition, at  $q^2 = 0$ , with the constraints  $G_E^n = 0$  and  $G_M^n = \mu_n$ ,  $G_E^p = 1$  and  $G_M^p = \mu_p$ , the coefficients  $f_1^n$ ,  $f_2^n$ ,  $f_1^p$  and  $f_2^p$  can be calculated,

$$f_1^n = \frac{\beta_\rho - \beta_\omega}{\sqrt{2}} + \frac{\beta_{\rho(2D)} - \beta_{\omega(3D)} - \beta_{\omega(5S)}}{\sqrt{2}}, \quad (15)$$

$$f_2^n = \mu_n - \frac{\alpha_\omega}{\sqrt{2}} + \frac{\alpha_{\rho(2D)} - \alpha_{\omega(3D)} - \alpha_{\omega(5S)}}{\sqrt{2}}, \quad (16)$$

$$f_1^p = 1 - \frac{\beta_\rho + \beta_\omega}{\sqrt{2}} - \frac{\beta_{\rho(2D)} + \beta_{\omega(3D)} + \beta_{\omega(5S)}}{\sqrt{2}}, \quad (17)$$

$$f_2^p = \mu_p - 1 - \frac{\alpha_\omega}{\sqrt{2}} - \frac{\alpha_{\rho(2D)} + \alpha_{\omega(3D)} + \alpha_{\omega(5S)}}{\sqrt{2}}, \quad (18)$$

with  $\mu_n = -1.91$  and  $\mu_p = 2.79$  as quoted in the PDG [57]. These coefficients  $\beta_\rho$ ,  $\beta_\omega$ ,  $\beta_{\rho(2D)}$ ,  $\beta_{\omega(3D)}$ ,  $\beta_{\omega(5S)}$ ,  $\alpha_\omega$ ,  $\alpha_{\rho(2D)}$ ,  $\alpha_{\omega(3D)}$ ,  $\alpha_{\omega(5S)}$  are model parameters, which will be determined by fitting them to the experimental data of the  $e^+e^- \rightarrow p\bar{p}$  and  $e^+e^- \rightarrow n\bar{n}$  reactions.

### III. NUMERICAL RESULTS

Under the above formulations, we perform the  $\chi^2$  fit to the experimental data of  $e^+e^- \rightarrow N\bar{N}$  reaction. There are 224 data points in total, with center-of-mass energies range from the kinematic reaction threshold to 3.2 GeV. These experimental data are: i) the total cross sections of  $e^+e^- \rightarrow N\bar{N}$  reaction from BESIII Collaboration [13, 15–18], CMD3 Collaboration [14], *BABAR* Collaboration [11], and SND Collaboration [12, 20, 65]; ii) the electromagnetic form factors  $|G_E|$  and  $|G_M|$  for nucleon from BESIII Collaboration [16, 66]; iii) the ratio of  $|G_E/G_M|$  from *BABAR* Collaboration [11], CMD3 Collaboration [14], and BESIII Collaboration [15, 17].

The results of the fitted parameters are listed in Table II. The corresponding  $\chi^2/\text{d.o.f}$  is 1.6, where d.o.f is the number of dimension of the freedom.

We show firstly the fitted numerical results of the electromagnetic form factors of proton and neutron in Fig. 1, comparing with the experimental data of the BESIII Collaboration. Within the contributions of the excited  $\rho(2D)$ ,  $\omega(3D)$ , and

TABLE II: Values of the fitted parameters.

Parameter	Value	Parameter	Value
$\beta_\rho$	$1.471 \pm 0.131$	$\alpha_\omega$	$-904.176 \pm 20.211$
$\beta_\omega$	$7.357 \pm 0.102$	$\alpha_{\rho(2D)}$	$0.601 \pm 0.101$
$\beta_{\rho(2D)}$	$-0.419 \pm 0.109$	$\alpha_{\omega(3D)}$	$-0.734 \pm 0.081$
$\beta_{\omega(3D)}$	$0.726 \pm 0.083$	$\alpha_{\omega(5S)}$	$0.313 \pm 0.028$
$\beta_{\omega(5S)}$	$-0.334 \pm 0.034$		

$\omega(5S)$  states, we can obtain a good description of the electromagnetic form factors for both proton and neutron. For the electric form factor of proton, there is a dip structure around 2.3 GeV which is because of the interference between the contributions of  $\omega(3D)$  and  $\omega(5S)$ , and there is a clear peak for the  $\omega(5S)$ . It is expected that these theoretical results can be tested by future experiments.

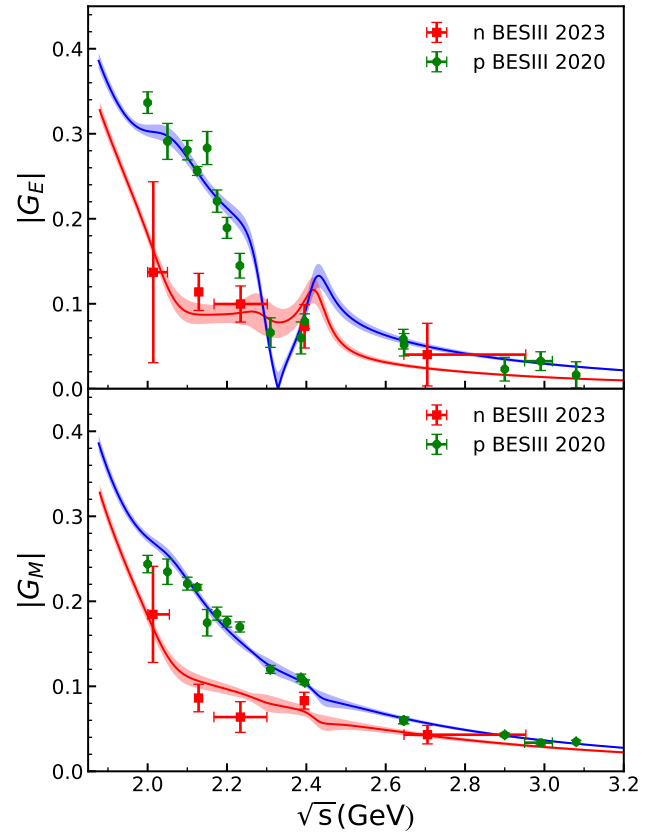


FIG. 1: Fitted results for the electromagnetic form factors of the proton and neutron comparing with the experimental data. The error bands are calculated with the uncertainties of the fitted parameters.

Second, we show the fitted results of the modulus of the ratio  $G_E/G_M$  for the proton in Fig. 2. The experimental data have large errors. Again, there are dip and bump structures because of the contributions of  $\omega(3D)$  and  $\omega(5S)$  states. It is worthy mentioning that the ratio of  $G_E/G_M$  equals to one at the reaction threshold as it should be. Clearly, more precise experimental data are needed to check our model calculations.

The fitted numerical results of the total cross sections of

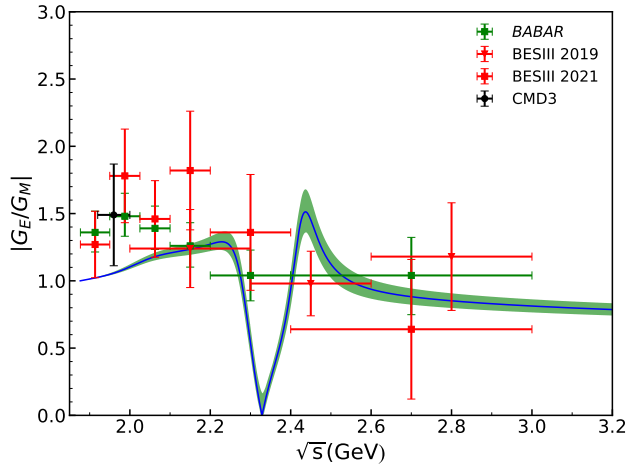


FIG. 2: The ratio  $|G_E/G_M|$  of proton.

$e^+e^- \rightarrow p\bar{p}$  and  $e^+e^- \rightarrow n\bar{n}$  reactions are shown in Figs. 3 (a) and (d), respectively. One can see that, thanks to the contribution of  $\rho(2D)$ , the platform behavior of the total cross section of  $e^+e^- \rightarrow p\bar{p}$  can be well reproduced, and the experimental data of the  $e^+e^- \rightarrow n\bar{n}$  can also be described within the fitted model parameters. Furthermore, these nonmonotonic structures around 2.2 to 2.4 GeV can be fairly well reproduced by considering the contributions of  $\omega(3D)$  and  $\omega(5S)$  states. In fact, a resonance with mass around 2300 MeV and width about 188 MeV is needed in the analysis of the total cross sections of  $e^+e^- \rightarrow p\bar{p}$  reaction in Ref. [26], where a simple Breit-Wigner amplitude for the  $e^+e^- \rightarrow p\bar{p}$  reaction was taken.

Since we can reproduce the total cross sections of  $e^+e^- \rightarrow p\bar{p}$  and  $e^+e^- \rightarrow n\bar{n}$  reactions, it is expected that the effective form factors of proton and neutron can also be described well, as shown in Figs. 3 (b) and (e), respectively. This indicates that the nonmonotonic line shapes of the nucleon effective form factors can be explained within the VMD model, where the contributions of the excited vector mesons are taken into account.

Next, we will discuss the nonmonotonic features of the nucleon effective form factors. In general, the main part of the effective form factors of the nucleon can be described by a dipole form as shown in Eq. (1) with a global factor  $c_0$ ,  $G_D = c_0/(1 - \gamma s)^2$ . By fitting the experimental data of the effective form factors of proton and neutron, we get  $c_0 = 5.54 \pm 0.02$  for proton and  $c_0 = 4.08 \pm 0.04$  for neutron. Then, subtracting the obtained effective form factor  $|G_{\text{eff}}|$  from  $G_D$ , one can get the residual  $G_{\text{osc}}$ ,

$$G_{\text{osc}} = |G_{\text{eff}}| - G_D = |G_{\text{eff}}| - \frac{c_0}{(1 - \gamma s)^2}. \quad (19)$$

The predictions of our model for the oscillation parts of the nucleon effective form factors are shown in Figs. 3 (c) and (f), respectively. It is found that the model predictions are in agreement with the subtracted data obtained with Eq. (19).

Note that, in Ref. [18], to get the conclusion which the effective form factor of both proton and neutron show a periodic behaviour, different formula of  $G_D$  were taken for proton and neutron. A three-pole formula  $F_{3p} = F_0/[(1+s/s_0)(1-\gamma s)^2]$  with  $s_0 = 8.8 \text{ GeV}^2$  were used for the case of proton [5, 31], while the above dipole formula was used for neutron. In this work, we take the same formula for both proton and neutron. From the results shown in Figs. 3 (c) and (f), it is difficult to conclude the oscillation behaviour of the effective form factors of nucleon.<sup>2</sup>

Now we turn to the ratio of the total cross sections of  $e^+e^- \rightarrow p\bar{p}$  and  $e^+e^- \rightarrow n\bar{n}$  reactions. Until a few years ago, there had been some pioneering experimental efforts dedicated to the  $e^+e^- \rightarrow n\bar{n}$  reaction by the FENICE experiment [67]. Even though the experimental data have large errors, and it is found that the total cross section of  $e^+e^- \rightarrow n\bar{n}$  reaction is twice as large as the one of  $e^+e^- \rightarrow p\bar{p}$  reaction, which is quite difficult to understand, since most theoretical predictions are opposite.

Very recently, the BESIII Collaboration has published a new precise measurement of the total cross sections of  $e^+e^- \rightarrow n\bar{n}$  reaction [18], and it is found that the ratio  $R = \sigma_{e^+e^- \rightarrow p\bar{p}}/\sigma_{e^+e^- \rightarrow n\bar{n}}$  is larger than 1 at all the measured energies, which is contrast to the results obtained by the FENICE experiment. The new results of BESIII Collaboration indicates that the photon-proton coupling is stronger than the corresponding photon-neutron coupling. The SND Collaboration also measured the total cross sections of  $e^+e^- \rightarrow n\bar{n}$  reaction with 2123 selected  $n\bar{n}$  events for 14 energy points [20] and their experimental results are consistent with the results of BESIII Collaboration.

Our theoretical results are shown in Fig. 4 by blue curve with error bands obtained from the uncertainties of the fitted parameters. The experimental data taken from BESIII and FENICE are also shown. Again, we can describe quite well the new experimental data by BESIII Collaboration [18].

#### IV. SUMMARY

In this work, we study the effective form factors of proton and neutron in the timelike region using a phenomenological extending vector meson dominance model. In addition to the contribution of the ground states  $\rho$  and  $\omega$ , the contributions from three theoretical predicted vector states  $\rho(2D)$ ,  $\omega(3D)$ , and  $\omega(5S)$  are also taken into account. It is found that we can successfully describe the cross sections of  $e^+e^- \rightarrow p\bar{p}$  and  $e^+e^- \rightarrow n\bar{n}$  reactions and also the effective form factors for both proton and neutron. Furthermore, the electromagnetic

<sup>2</sup> Same result is obtained if we used the three-pole formula for both proton and neutron. The dipole form was firstly obtained from the best fit to the electromagnetic form factors of proton in the space-like region. Nevertheless, the VMD model and the dipole form of  $g(q^2)$  can give a reasonable description of the experimental data on the baryon EMFFs at the considered energy region.

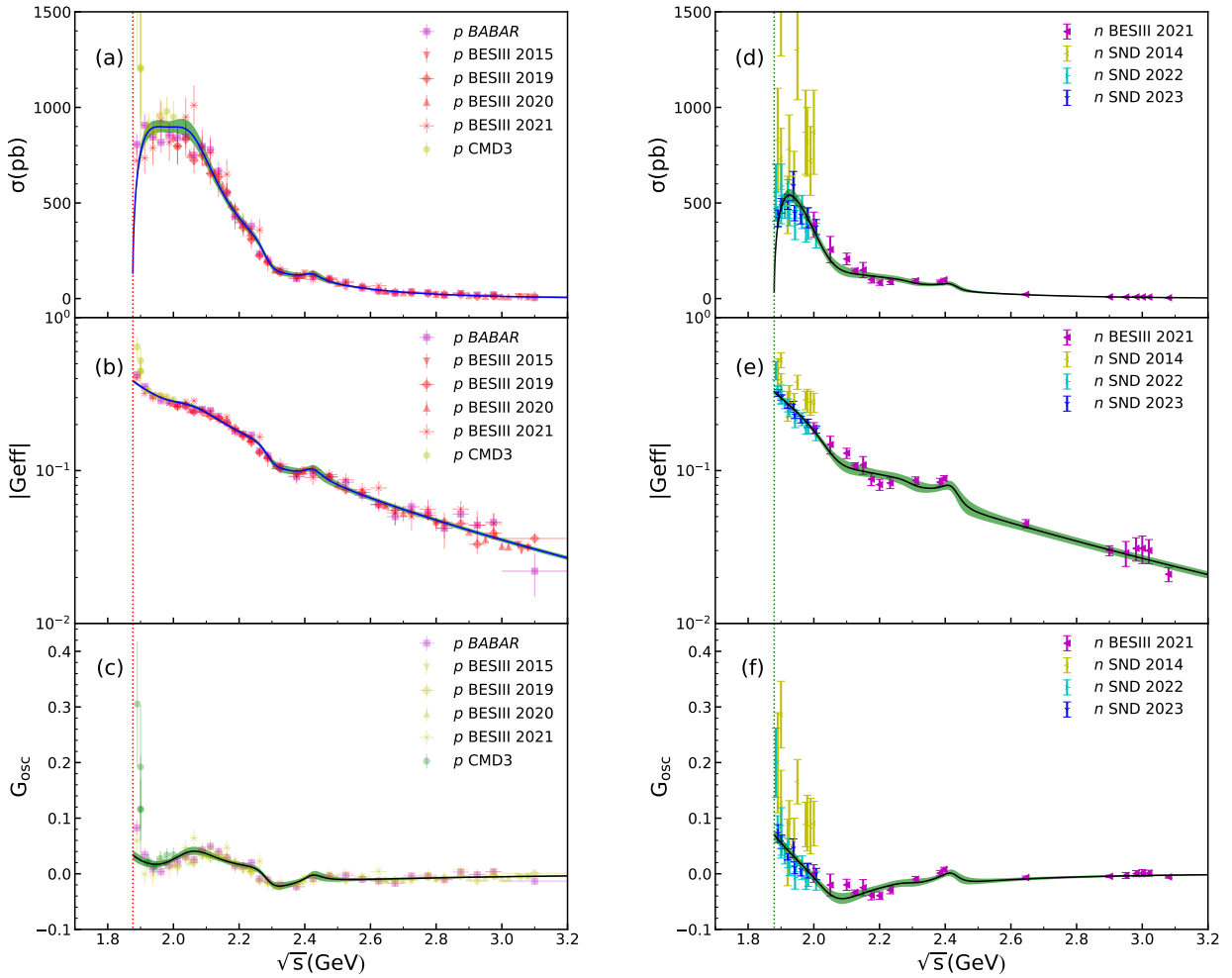


FIG. 3: The fitted results of total cross sections, effective form factors, and the oscillation part of the effective form factors for proton (left) and neutron (right). These error bands are obtained with the uncertainties of the fitted parameters. The red and green vertical dotted curves represent the  $e^+e^- \rightarrow p\bar{p}$  and  $n\bar{n}$  kinematic reaction threshold, respectively.

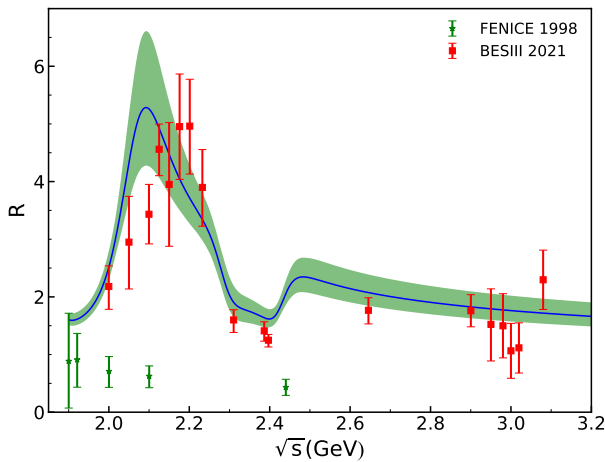


FIG. 4: The ratio  $R = \sigma_{e^+e^- \rightarrow p\bar{p}}/\sigma_{e^+e^- \rightarrow n\bar{n}}$  as a function of  $\sqrt{s}$  compared with the experimental data.

form factors and the modulus of their ratio can be also obtained, which are in agreement with the experimental data. In addition, thanks to the contributions from the excited vector resonances and the phenomenological dipole formula for the intrinsic form factor  $g(s) = 1/(1 - \gamma s)^2$ , the flat behaviour of the nucleon effective form factors around the threshold can be reproduced, and we are able to provide a natural explanation for the nonmonotonic behavior which was found in the time-like nucleon electromagnetic form factors.

Our study here shows that the so-called periodic behaviour of the nucleon effective form factors is not confirmed. However, there are indeed nonmonotonic structures in the line shape of nucleon effective form factors, which can be naturally reproduced by considering the contributions from the low-lying excited vector states. We hope that our present work can stimulate more studies along this line, and it is expected that more precise future experimental measurements, especially for the case of the  $e^+e^- \rightarrow n\bar{n}$  reaction, can be used to check our model calculations.

Finally, we would like to stress that, thanks to the impor-

tant role played by the excited vector states contribution in the  $e^+e^- \rightarrow N\bar{N}$  reaction, accurate data for this reaction can be used to improve our knowledge of those low-lying excited vector states above 2 GeV, which are at present poorly known. This work constitutes a first step in this direction.

### ACKNOWLEDGEMENTS

We would like to thank Dr. Lei Xia for useful discussions. This work is partly supported by the National Natural Sci-

ence Foundation of China under Grant No. 12075288. It is also supported by the Youth Innovation Promotion Association CAS.

- 
- [1] S. Pacetti, R. Baldini Ferroli, and E. Tomasi-Gustafsson, *Phys. Rept.* **550-551**, 1 (2015).
- [2] M. A. Belushkin, H. W. Hammer, and U. G. Meissner, *Phys. Rev. C* **75**, 035202 (2007), hep-ph/0608337.
- [3] E. A. Kuraev, E. Tomasi-Gustafsson, and A. Dbeyssi, *Phys. Lett. B* **712**, 240 (2012), 1106.1670.
- [4] A. Bianconi and E. Tomasi-Gustafsson, *Phys. Rev. Lett.* **114**, 232301 (2015), 1503.02140.
- [5] E. Tomasi-Gustafsson, A. Bianconi, and S. Pacetti, *Phys. Rev. C* **103**, 035203 (2021), 2012.14656.
- [6] O. Gayou et al. (Jefferson Lab Hall A), *Phys. Rev. Lett.* **88**, 092301 (2002), nucl-ex/0111010.
- [7] O. Gayou et al., *Phys. Rev. C* **64**, 038202 (2001).
- [8] L. Andivahis et al., *Phys. Rev. D* **50**, 5491 (1994).
- [9] P. E. Bosted et al., *Phys. Rev. Lett.* **68**, 3841 (1992).
- [10] M. K. Jones et al. (Jefferson Lab Hall A), *Phys. Rev. Lett.* **84**, 1398 (2000), nucl-ex/9910005.
- [11] J. P. Lees et al. (BaBar), *Phys. Rev. D* **87**, 092005 (2013), 1302.0055.
- [12] M. N. Achasov et al., *Phys. Rev. D* **90**, 112007 (2014), 1410.3188.
- [13] M. Ablikim et al. (BESIII), *Phys. Rev. D* **91**, 112004 (2015), 1504.02680.
- [14] R. R. Akhmetshin et al. (CMD-3), *Phys. Lett. B* **759**, 634 (2016), 1507.08013.
- [15] M. Ablikim et al. (BESIII), *Phys. Rev. D* **99**, 092002 (2019), 1902.00665.
- [16] M. Ablikim et al. (BESIII), *Phys. Rev. Lett.* **124**, 042001 (2020), 1905.09001.
- [17] M. Ablikim et al. (BESIII), *Phys. Lett. B* **817**, 136328 (2021), 2102.10337.
- [18] M. Ablikim et al. (BESIII), *Nature Phys.* **17**, 1200 (2021), 2103.12486.
- [19] G. Huang and R. B. Ferroli (BESIII), *Natl. Sci. Rev.* **8**, nwab187 (2021), 2111.08425.
- [20] M. N. Achasov et al. (SND), *Eur. Phys. J. C* **82**, 761 (2022), 2206.13047.
- [21] R.-G. Ping, *Chin. Phys. C* **38**, 083001 (2014), 1309.3932.
- [22] M. Ablikim et al. (BESIII), *Chin. Phys. C* **41**, 063001 (2017), 1702.04977.
- [23] M. Ablikim et al. (BESIII), *Chin. Phys. C* **41**, 113001 (2017), 1705.09722.
- [24] Y.-H. Lin, H.-W. Hammer, and U.-G. Meißner, *Phys. Rev. Lett.* **128**, 052002 (2022), 2109.12961.
- [25] X. Cao, J.-P. Dai, and H. Lenske, *Phys. Rev. D* **105**, L071503 (2022), 2109.15132.
- [26] L. Xia, C. Rosner, Y. D. Wang, X. Zhou, F. E. Maas, R. B. Ferroli, H. Hu, and G. Huang, *Symmetry* **14**, 231 (2022), 2111.13009.
- [27] A.-X. Dai, Z.-Y. Li, L. Chang, and J.-J. Xie, *Chin. Phys. C* **46**, 073104 (2022), 2112.06264.
- [28] A. Bianconi and E. Tomasi-Gustafsson, *Phys. Rev. C* **105**, 065206 (2022), 2204.05197.
- [29] Q.-H. Yang, L.-Y. Dai, D. Guo, J. Haidenbauer, X.-W. Kang, and U.-G. Meißner (2022), 2206.01494.
- [30] A. I. Milstein and S. G. Salnikov, *Phys. Rev. D* **106**, 074012 (2022), 2207.14020.
- [31] E. Tomasi-Gustafsson and S. Pacetti, *Phys. Rev. C* **106**, 035203 (2022).
- [32] R.-Q. Qian, Z.-W. Liu, X. Cao, and X. Liu, *Phys. Rev. D* **107**, L091502 (2023), 2211.11555.
- [33] J.-P. Dai, X. Cao, and H. Lenske, *Phys. Lett. B* **846**, 138192 (2023), 2304.04913.
- [34] E. L. Lomon and S. Pacetti, *Phys. Rev. D* **85**, 113004 (2012), [Erratum: *Phys. Rev. D* **86**, 039901 (2012)], 1201.6126.
- [35] M. Ablikim et al. (BESIII) (2019), 1912.11208.
- [36] M. Ablikim et al. (BESIII), *Phys. Rev. D* **103**, 072007 (2021), 2012.07360.
- [37] M. Ablikim et al. (BESIII), *Phys. Rev. D* **104**, 032007 (2021), 2104.05549.
- [38] M. Ablikim et al. (BESIII), *Phys. Rev. D* **104**, 092014 (2021), 2105.13597.
- [39] M. Ablikim et al. (BESIII), *Phys. Rev. D* **100**, 032009 (2019), 1907.06015.
- [40] M. Ablikim et al. (BESIII), *Phys. Rev. D* **102**, 012008 (2020), 2003.13064.
- [41] M. Ablikim et al. (BESIII), *Phys. Rev. D* **99**, 032001 (2019), 1811.08742.
- [42] M. Ablikim et al. (BESIII), *Phys. Rev. Lett.* **124**, 112001 (2020), 2001.04131.
- [43] M. Ablikim et al. (BESIII), *Phys. Lett. B* **813**, 136059 (2021), 2009.08099.
- [44] F. Iachello, A. D. Jackson, and A. Lande, *Phys. Lett. B* **43**, 191 (1973).
- [45] F. Iachello and Q. Wan, *Phys. Rev. C* **69**, 055204 (2004).
- [46] R. Bijker and F. Iachello, *Phys. Rev. C* **69**, 068201 (2004), nucl-th/0405028.
- [47] B. Yan, C. Chen, and J.-J. Xie, *Phys. Rev. D* **107**, 076008 (2023), 2301.00976.
- [48] A. Bianconi and E. Tomasi-Gustafsson, *Phys. Rev. C* **93**, 035201 (2016), 1510.06338.
- [49] Y. Yang, D.-Y. Chen, and Z. Lu, *Phys. Rev. D* **100**, 073007 (2019), 1902.01242.
- [50] Z.-Y. Li, A.-X. Dai, and J.-J. Xie, *Chin. Phys. Lett.* **39**, 011201

- (2022), 2107.10499.
- [51] L.-M. Wang, J.-Z. Wang, and X. Liu, *Phys. Rev. D* **102**, 034037 (2020), 2007.03118.
- [52] Q.-S. Zhou, J.-Z. Wang, X. Liu, and T. Matsuki, *Phys. Rev. D* **105**, 074035 (2022), 2201.06393.
- [53] J.-Z. Wang, L.-M. Wang, X. Liu, and T. Matsuki, *Phys. Rev. D* **104**, 054045 (2021), 2106.14582.
- [54] L.-M. Wang, S.-Q. Luo, and X. Liu, *Phys. Rev. D* **105**, 034011 (2022), 2109.06617.
- [55] Q.-T. Song, D.-Y. Chen, X. Liu, and T. Matsuki, *Phys. Rev. D* **91**, 054031 (2015), 1501.03575.
- [56] L.-P. He, X. Wang, and X. Liu, *Phys. Rev. D* **88**, 034008 (2013), 1306.5562.
- [57] R. L. Workman et al. (Particle Data Group), *PTEP* **2022**, 083C01 (2022).
- [58] B. Aubert et al. (BaBar), *Phys. Rev. D* **73**, 012005 (2006), hep-ex/0512023.
- [59] S. Dobbs, A. Tomaradze, T. Xiao, K. K. Seth, and G. Bonvicini, *Phys. Lett. B* **739**, 90 (2014), 1410.8356.
- [60] J. Haidenbauer, X. W. Kang, and U. G. Meißner, *Nucl. Phys. A* **929**, 102 (2014), 1405.1628.
- [61] A. B. Arbuzov and T. V. Kopylova, *JHEP* **04**, 009 (2012), 1111.4308.
- [62] M. Irshad, D. Liu, X. Zhou, and G. Huang, *Symmetry* **14**, 69 (2022).
- [63] R. G. Sachs, *Phys. Rev.* **126**, 2256 (1962).
- [64] J. R. Green, J. W. Negele, A. V. Pochinsky, S. N. Syritsyn, M. Engelhardt, and S. Krieg, *Phys. Rev. D* **90**, 074507 (2014), 1404.4029.
- [65] M. N. Achasov et al. (SND) (2023), 2309.05241.
- [66] M. Ablikim et al. (BESIII), *Phys. Rev. Lett.* **130**, 151905 (2023), 2212.07071.
- [67] A. Antonelli et al., *Nucl. Phys. B* **517**, 3 (1998).